Development 135, 973-982 (2008) doi:10.1242/dev.015438

The *Drosophila* hnRNP M homolog Rumpelstiltskin regulates *nanos* mRNA localization

Roshan A. Jain* and Elizabeth R. Gavis†

Anterior-posterior axis patterning of the *Drosophila* embryo requires Nanos activity selectively in the posterior. This spatial asymmetry of Nanos is generated by the localization of *nanos* mRNA to the posterior pole of the embryo, where it is subsequently translated. Posterior localization of *nanos* is mediated by a complex cis-acting localization signal in its 3′ untranslated region comprising several partially redundant localization elements. This localization signal redundancy has hampered the identification of trans-acting factors that act specifically to effect posterior localization of *nanos*. Here, we have used a biochemical approach to identify Rumpelstiltskin, a *Drosophila* heterogeneous nuclear ribonucleoprotein (hnRNP) M homolog, which binds directly to an individual *nanos* localization element. Rumpelstiltskin associates with *nanos* mRNA in vitro and in vivo, and binding by Rumpelstiltskin correlates with localization element function in vivo. Through analysis of a *rumpelstiltskin* null mutation by genetic strategies that circumvent redundancy, we demonstrate that Rumpelstiltskin regulates anterior-posterior axis patterning by functioning as a direct-acting *nanos* mRNA localization factor.

KEY WORDS: *Drosophila*, hnRNP, mRNA localization, Nanos

INTRODUCTION

The anterior-posterior body axis of the *Drosophila* embryo is established through the asymmetric distribution of Bicoid (Bcd) and Nanos (Nos) proteins, which form gradients emanating from the anterior and posterior poles of the embryo, respectively (Driever and Nüsslein-Volhard, 1988; Gavis and Lehmann, 1992). Bcd functions as a transcriptional activator and a translational repressor to regulate expression of genes required for head and thorax development (Driever and Nüsslein-Volhard, 1989; Dubnau and Struhl, 1996; Rivera-Pomar et al., 1996; Struhl et al., 1989). As a translational regulator, Nos represses synthesis of the transcriptional repressor Hunchback (Hb) in the posterior of the embryo, permitting expression of genes required for abdominal development (Hülskamp and Tautz, 1991; Tautz and Pfeifle, 1989). More recently, additional roles for Nos have been identified in germline stem cell divisions, germ cell development, and dendrite morphogenesis (Forbes and Lehmann, 1998; Kobayashi et al., 1996; Wang and Lin, 2004; Ye et al., 2004).

The Bcd and Nos protein asymmetries are generated through the asymmetric localization and consequent translation of their respective mRNAs (Berleth et al., 1988; Driever and Nüsslein-Volhard, 1988; Gavis and Lehmann, 1992; Wang and Lehmann, 1991). Both *bcd* and *nos* mRNAs are synthesized maternally and become localized to opposite poles of the egg during oogenesis. Whereas anterior localization of *bcd* depends on active transport along microtubules (Cha et al., 2001; Weil et al., 2006), posterior localization of *nos* occurs by passive diffusion and entrapment at the posterior by the specialized posterior cytoplasm or germ plasm (Forrest and Gavis, 2003; Weil et al., 2006). Localization of *nos* to the germ plasm is essential to activate *nos* translation and produce the critical concentration of Nos required to repress translation of *hb* mRNA (Gavis and Lehmann, 1992; Gavis and Lehmann, 1994). Thus, when *nos* localization is abolished by mutations in germ plasm components such as *oskar* (*osk*) or *vasa* (*vas*), Nos is not produced and the resulting embryos lack abdominal segments. Although *nos* is highly concentrated at the posterior of the embryo, its localization is inefficient, such that the majority of *nos* mRNA remains unlocalized (Bergsten and Gavis, 1999). The obligate linkage of *nos* mRNA localization and translation prevents synthesis of Nos in the anterior of the embryo, where it is deleterious to head and thorax development (Gavis and Lehmann, 1992; Gavis and Lehmann, 1994; Wharton and Struhl, 1989). Recently, posterior localization of *nos* has also been shown to be essential for *nos* function in germ cell development (Gavis et al., 2008).

bcd and *nos* are two of a growing number of mRNAs known to be localized within *Drosophila* oocytes and embryos. Since different mRNAs are targeted to different destinations, specificity for localization pathways must be encoded in the transcripts and conferred on the cellular localization machinery by factors that recognize these signals. Cis-acting sequences that direct intracellular localization have been identified in a number of localized mRNAs and are usually located in 3′ untranslated regions (3′UTRs) (Gavis et al., 2007; St Johnston, 2005). Posterior localization of *nos* mRNA is directed by a large localization signal within the *nos* 3′UTR that can be subdivided into four partially redundant localization elements (Gavis et al., 1996a). Individual localization elements exhibit varying degrees of competence to mediate posterior localization, but at least three contiguous elements are required to produce wild-type levels of Nos and proper abdominal development (Bergsten and Gavis, 1999). Such functional redundancy is characteristic of a variety of mRNA localization signals including the *bcd*, *Xenopus Vg1* and *fatvg*, and yeast *ASH1* signals (Chan et al., 1999; Gautreau et al., 1997; Gonzalez et al., 1999; Macdonald and Kerr, 1998).

Previous genetic and biochemical studies suggest that different *nos* localization elements are recognized by distinct cytoplasmic factors that package *nos* into a ribonucleoprotein (RNP) complex competent to interact with the germ plasm components (Bergsten and Gavis, 1999; Bergsten et al., 2001). However, the specific

Department of Molecular Biology, Princeton University, Princeton, NJ 08544, USA.

*Present address: Department of Cell and Developmental Biology, University of Pennsylvania, Philadelphia, PA 19104, USA
†Author for correspondence (e-mail: lgavis@princeton.edu)

Accepted 18 December 2007

localization factors that recognize the *nos* localization elements and target *nos* to the germ plasm have remained elusive. Although mutations that cause defects in *nos* localization have been identified in numerous genetic screens, the effects of these mutations on *nos* are most likely to be indirect, as they disrupt localization or assembly of germ plasm. A recent genetic screen for *nos* localization factors identified the chaperone Hsp90 (also known as Hsp83 – FlyBase) as being important for *nos* localization, though its role also appears to be indirect (Song et al., 2007). Given the redundancy within the *nos* localization signal and, consequently, the potential for functional redundancy among proteins that interact with different *nos* localization elements, genetic approaches may fail to identify direct-acting localization factors.

We have therefore taken a biochemical approach to identify *nos* localization factors, starting with an individual *nos* localization element. Using a new RNA-affinity purification strategy, we have isolated Rumpelstiltskin (Rump), a member of the heterogeneous nuclear ribonucleoprotein (hnRNP) family. Rump appears to be the *Drosophila* homolog of hnRNP M (also known as HNRPM in mouse), which has been previously implicated as a splicing factor in both invertebrates and vertebrates (Gattoni et al., 1996; Hase et al., 2006). A combination of biochemical and genetic data presented here show that Rump is a direct-acting *nos* mRNA localization factor. Rump associates with *nos* mRNA in vivo and binding of Rump to *nos* mRNA in vitro requires a repeated motif within the *nos* localization signal. Moreover, binding of Rump in vitro correlates with the ability of this motif to confer localization function in vivo. Through the analysis of a *rump* null mutant, we demonstrate a specific role for *rump* in posterior localization of *nos*. To our knowledge, this is the first example of an hnRNP M homolog regulating the localization of an mRNA target.

MATERIALS AND METHODS

Tandem RNA affinity purification (TRAP) of Rump

Three tandem copies of the *nos* +2′ localization element (Bergsten and Gavis, 1999) were cloned into the *Bgl*II site of pTRAP6 (gift of H. Krause, University of Toronto, Toronto, Canada) to generate pTRAP6-nos+2′-3X. pTRAP6 and pTRAP6-nos+2′-3X were linearized with *Sca*I and *Hin*dIII, respectively, for in vitro transcription by the mMessage mMachine Kit (Ambion) supplemented with 625 nM [α-^{32}P]UTP. Radiolabeled capped TRAP+2′-3X (779 nucleotide) and TRAP-ctrl (1261 nucleotide) RNAs were purified by G-50 Sephadex Quick Spin Column (Roche). MCP was cloned from pCaS-P_{hsp83}-MCP-GFP (Forrest and Gavis, 2003) into pGEX-4T-1, fusing MCP to the C-terminus of GST. GST-MCP was purified after expression in *E. coli* using glutathione-agarose (Sigma) according to the manufacturer's instructions.

Extract was prepared from 0- to 2-hour Oregon R embryos in TPB [60 mM HEPES pH 7.5, 10 mM $MgCl_2$, 150 mM NaCl, 0.1% Triton X-100, 10% glycerol, 1× EDTA-free Complete Protease Inhibitors (Roche)] as described (Bergsten et al., 2001). All subsequent purification steps were performed at 4°C. For each sample, 1 ml of extract (5 mg/ml total protein) was precleared with 40 μl streptavidin-agarose and 40 μl glutathione-agarose for 30 minutes. Precleared extract was incubated with 11 μg radiolabeled TRAP-ctrl or TRAP+2′-3X RNA for 15 minutes, then rotated with 200 μl streptavidin-agarose in a 1.2 ml RNase-free minicolumn (BioRad) for 2 hours. The resin was washed with 25 volumes of TPB and bound RNP complexes were eluted by incubation with 5 mM D-biotin in TPB for 1 hour, with a second elution for 30 minutes. The eluates were pooled and incubated with 100 μl glutathione-agarose pre-bound with 1 mg GST-MCP for 2 hours with rotation. The resin was washed with 15 volumes of TPB and proteins were eluted by treatment with 2 μg RNase A in 200 μl TPB, 2× 30 minutes. Eluates were pooled, concentrated by TCA precipitation, then resuspended in boiling sample buffer (Gavis et al., 1996b). Samples were separated by SDS-PAGE, with the amount of each sample loaded adjusted for the amount of RNA captured, as determined by scintillation counting. Proteins were visualized by SYPRO Ruby (Invitrogen) staining, and the indicated ~70 kDa band was excised and analyzed by mass spectrometry.

Production of MBP-Rump

The full-length *rump* coding region was amplified by RT-PCR from 0- to 2-hour Oregon R embryonic poly(A$^+$) RNA using the primers 5′-AAACT-GCAGAGCATGGACGCTAGTAAC-3′ and 5′-CCCAAGCTTAAAAG-TATGTTAC-3′, which introduce *Pst*I and *Hin*dIII sites at the 5′ and 3′ ends, respectively. Following digestion with *Pst*I and *Hin*dIII, the PCR fragment was inserted between the *Pst*I and *Hin*dIII sites of pMAL-c2 (New England Biolabs), fusing Rump to the C-terminus of MBP. MBP-Rump was expressed and purified on amylose-agarose (Kalifa et al., 2006), exchanged into Storage Buffer (100 mM KCl, 25 mM HEPES pH 7.9, 0.5 mM EDTA, 10% glycerol, 1 mM DTT, 0.5 mM PMSF), and stored at –80°C. For monoclonal antibody production, the MBP tag was removed using Factor Xa (a gift from F. Hughson, Princeton University, Princeton, NJ).

UV-crosslinking assay

Radiolabeled RNA probe synthesis and UV-crosslinking were performed as previously described using 27 μg MBP-Rump per reaction (Bergsten et al., 2001). The full-length +2′ element [nucleotides 101-186 of the *nos* 3′UTR (Gavis et al., 1996a)] was inserted between the *Sma*I and *Bam*HI sites of the pBluescript derivative pBS-SKΔKP (Kalifa et al., 2006). The +2′ element deletions (Δ1, nucleotides 101-128; Δ2, 101-142; Δ3, 120-162; Δ4, 128-152; Δ5, 144-186) were generated by PCR (Δ1-3, Δ5) or with annealed oligos (Δ4) and cloned into pBS-SKΔKP as above. The +2′(A)G:C, +2′(D)G:C and +2′(AD)G:C mutants were generated by PCR, introducing G-to-C point mutations into one or both of the two CGUU motifs (A, *nos* 3′UTR nucleotide 120; D, nucleotide 140] in the pBS-SKΔKPnos+2′ plasmid. Plasmids were linearized with *Bam*HI for probe synthesis. For immunoprecipitation of crosslinked protein, each RNase-treated reaction was incubated for 1 hour at 4°C in 200 μl IP buffer (10 mM Tris-HCl pH 7.4, 100 mM NaCl, 2.5 mM $MgCl_2$, 0.5% Triton X-100, 1 mM DTT, 1× EDTA-free Complete Protease Inhibitors) with 6 μl Protein-G Dynabeads (Invitrogen) coated with 30 μl antibody. Beads were washed twice with IP buffer, then resuspended directly in boiling sample buffer and separated by SDS-PAGE.

Generation of a *rump* null mutation

The *rump^1* allele was generated by imprecise excision of *P* element P{SUPor-P} CG9373^{KG02834} (Bellen et al., 2004). Excisions in trans to *Df(3R)by416*, which deletes the *rump* locus, were screened by single-fly PCR (Mansfield et al., 2002) using primer pairs to amplify the genomic regions immediately upstream and downstream of the *P* element insertion site. Genomic deletions were identified by the absence of a PCR product. The *rump^1* deletion endpoints were determined by PCR amplification with primers flanking the deletion and sequencing. The *nos^{BN}* allele (Wang et al., 1994) was recombined onto the *rump^1* and *Df(3R)by416* chromosomes to generate *rump^1 nos^{BN}* and *Df(rump) nos^{BN}* chromosomes used for the analysis of *nos-tub:nos+2* in Fig. 7.

Transgenes

The *nos-tub:nos+2* transgene is described by Gavis et al. (Gavis et al., 1996a). The *nos-tub:nos+2(A)G:C* and *nos-tub+2(D)G:C* transgenes are identical to *nos-tub:nos+2* except that a G-to-C mutation was introduced into the first (A) or second (D) CGUU motif within the +2′ sequences, using PCR. The *rump* rescue transgene contains a 6.5 kb *Ban*II genomic fragment from BACR19N07 (GenBank AC009350) containing *rump* inserted into pCaSpeR4. The *rump* transgene was introduced into *y w^{67c23}* embryos by *P* element-mediated germline transformation (Spradling, 1986) and multiple independent lines were isolated.

Northern blotting and immunoblotting

Northern blotting and immunoblotting were performed as previously described (Kalifa et al., 2006). A ^{32}P-labeled probe for *rump* was generated by random-hexamer labeling of the full-length *rump* EST clone GH11495. For immunoblotting, anti-Rump 5G4 was used at 1:2000, anti-Snf (gift of P. Schedl, Princeton University, Princeton, NJ) at 1:20,000. Proteins were detected using Lumi-Light Western Blot Substrate (Roche).

RNA co-immunoprecipitation

Ovaries from well-fed females were dissected in Schneider's medium (Invitrogen), rinsed with PBS and frozen in liquid N_2. Approximately 15 mg ovaries or dechorionated embryos per sample were homogenized on ice in 750 μl RNase-free RNA co-immunoprecipitation buffer (RCB) [50 mM HEPES pH 7.4, 200 mM NaCl, 2.5 mM $MgCl_2$, 0.1% Triton X-100, 250 mM sucrose, 1 mM DTT, 1× EDTA-free Complete Protease Inhibitors, 0.4 mM Pefabloc (Roche)], supplemented with 300 U RNasin (Promega). Subsequent steps were carried out at 4°C. Soluble extract was obtained by two sequential 5-minute centrifugations at 16,000 ***g***, then precleared with 40 μl Protein-G Dynabeads for 30 minutes at 4°C. After removal of samples for immunoblotting and quantitation of RNA input, Rump was immunoprecipitated from 450 μl precleared extract by incubation for 1 hour with 20 μl Protein-G Dynabeads bound with anti-Rump 5G4 antibody. Immunoprecipitates were washed eight times with RCB. Half of the IP was resuspended in RCB, treated with 8 units RQ1 RNase-free DNase (Promega) for 10 minutes at room temperature, then extracted with phenol:chloroform. RNA was ethanol precipitated with 30 μg tRNA and 5 μg glycogen as carrier and resuspended in DEPC-treated distilled H_2O for RT-PCR. The remainder of the IP was resuspended in 20 μl boiling sample buffer for immunoblotting.

For RT-PCR analysis, RNA samples were denatured for 3 minutes at 80°C, then chilled on ice. Half the denatured RNA was reverse transcribed using SuperScript II (Invitrogen) and oligo$(dT)_{15}$ for 2 hours at 42°C. The remaining half was treated similarly, except that SuperScript II was omitted. Thirty cycles of PCR amplification with Taq polymerase were performed using *nos* primers (5′-GCGATCAAGGCGGAATCG-3′ and 5′-ATAG-GATCCGAAAGTGTTCCTTGCTA-3′).

Embryonic cuticle preparation, in situ hybridization and immunostaining

Embryonic cuticle preparation and in situ hybridization were performed according to Gavis and Lehmann (Gavis and Lehmann, 1992). The statistical significance of embryonic phenotypes was determined by the χ^2 test. Immunostaining of ovaries was performed as previously described (Shcherbata et al., 2004). Embryo immunostaining was performed as described (Duchow et al., 2005), except that for anti-Rump immunofluorescence, dechorionated embryos were heat-fixed in 68 mM NaCl/0.03% Triton X-100, transferred to PBS, and the vitelline membranes were manually removed using a 30-gauge needle. The following antibodies and dyes were used: 1:100 anti-Rump 10C3 (immunofluorescence), 1:100 anti-Rump 5G4 (immunohistochemistry), 1:10,000 rabbit anti-Vas (gift of R. Lehmann, Skirball Institute, New York), 1:1000 Alexa Fluor 568 goat anti-mouse (Invitrogen/Molecular Probes), 1:1000 Alexa Fluor 488 goat anti-rabbit (Invitrogen/Molecular Probes), 1:1000 Oregon Green 488 phalloidin (Invitrogen/Molecular Probes), 1:1000 Hoechst (ovaries), 1:1000 DAPI (embryos). Images were obtained using standard Nomarksi optics or a Zeiss LSM510 confocal microscope.

RESULTS

Purification and identification of Rumpelstiltskin

To identify candidate *nos* regulatory factors, we used a two-step tandem RNA affinity purification (TRAP) method (Nelson et al., 2007) to isolate in vitro-assembled RNA-protein complexes containing the 88 nucleotide *nos* +2′ localization element. We focused on this element because previous mutational analysis suggested it as a target for multiple localization factors, and biochemical experiments identified a +2′ element binding activity of ~75 kDa (p75) in ovarian and embryonic extracts (Bergsten et al., 2001). In vitro-synthesized RNA containing the dual TRAP purification tags and three tandem copies of the +2′ element (TRAP+2′-3X; Fig. 1A) was allowed to form RNA-protein complexes with early (0- to 2-hour) embryonic protein extract. These complexes were isolated first on streptavidin resin, utilizing the specific interaction between streptavidin and the S1 RNA aptamer of the TRAP tag. Bound complexes were eluted by the addition of D-biotin and applied to glutathione resin coated with GST-MS2 coat protein (GST-MCP), which captures TRAP-tagged RNA through the interaction of GST-MCP with the six MCP-binding stem-loops present in the tag. This second purification step served to reduce non-specific background proteins that interact with the streptavidin-coated agarose beads. Subsequent RNase digestion allowed specific elution of the protein components of the recaptured RNP complexes and eluted proteins were separated by SDS-PAGE. To control for the isolation of non-specific RNA-binding proteins, an RNA of similar length containing naïve sequence in place of the *nos* regulatory sequences (TRAP-ctrl; Fig. 1A) was used in a parallel purification.

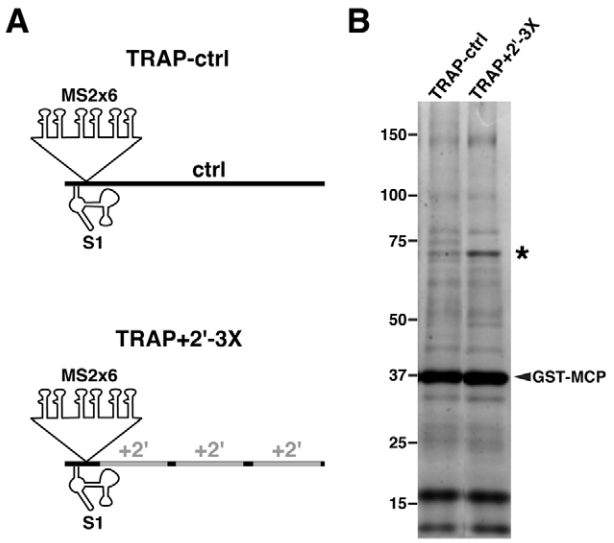

Fig. 1. Isolation of *Drosophila* Rump by tandem RNA-affinity purification. (**A**) TRAP-tagged RNAs with the streptavidin-binding S1 aptamer and six tandem copies of the MS2 stem-loop (MS2x6). TRAP+2′-3X RNA contains three tandem copies of the *nos* +2′ localization element, whereas the TRAP-ctrl RNA contains transcribed vector sequence. (**B**) SYPRO Ruby-stained SDS-PAGE gel showing the final RNase eluates from purifications performed in parallel with TRAP+2′-3X and TRAP-ctrl RNAs. The protein band enriched for Rump is marked with an asterisk. The faint band of similar size in the control purification contains contaminating *E. coli* Hsp70. GST-MCP that elutes non-specifically is marked with an arrowhead. To permit comparison between the two samples, the amount of protein eluate loaded was adjusted according to the pre-elution RNA recovery for each sample. Molecular mass standards are indicated in kDa.

A band of ~70 kDa was enriched by the TRAP+2′-3X RNA across several independent purifications (Fig. 1B and data not shown). In each case, this band was excised and the protein components were analyzed by mass spectrometry. Sixteen peptides were recovered spanning the 633 amino acids of a predicted 67 kDa protein encoded by the gene CG9373. The less intense band of ~70 kDa present in the TRAP-ctrl sample corresponds to the *E. coli* Hsp70 chaperone, a contaminant of the GST-MCP protein preparation (data not shown).

CG9373 encodes the *Drosophila* homolog of the human hnRNP M family of nucleic acid-binding proteins and is orthologous to the 59 kDa splicing factor Hrp59 of *Chironomus tentans* (Kiesler et al., 2005). Like other hnRNP M family members, the *Drosophila* homolog contains three RNA recognition motifs (RRMs). Based on cross-reactivity of antibodies against the *C. tentans* protein with a

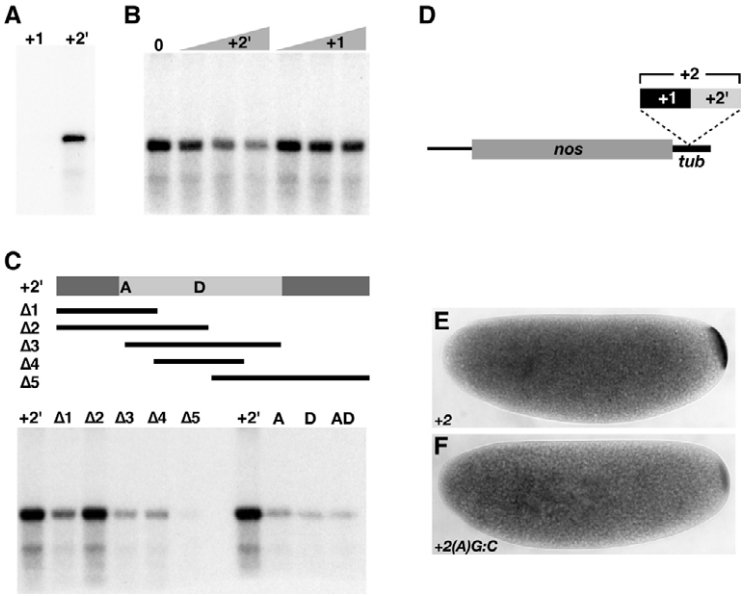

Fig. 2. Recognition by Rump correlates with *nos* RNA localization signal function. (**A**) UV-crosslinking of MBP-Rump to radiolabeled *nos* +1 and +2′ element RNA probes. (**B**) UV-crosslinking of MBP-Rump to radiolabeled +2′ element RNA in the absence (0) or presence of 200-, 400- and 600-fold molar excess of unlabeled +2′ or +1 element RNA. (**C**) Above is a diagram of the +2′ element with the two CGUU motifs (A and D) indicated. The lightly shaded region is highly conserved between *D. melanogaster* and *D. virilis* (Bergsten et al., 2001). The portions of the +2′ element retained in the deletion mutants (Δ1-5) are indicated by solid bars. C-to-G point mutations in the CGUU motifs were introduced individually (A or D) or in combination (AD) into the full-length +2′ element. Beneath is shown UV-crosslinking of MBP-Rump to the indicated radiolabeled RNA probes. (**D**) Diagram of the *nos-tub:nos+2* transgene, which contains only the *nos* +1 and +2′ localization elements. (**E**,**F**) In situ hybridization to *nos* in preblastoderm nos^{BN} embryos carrying (E) the *nos-tub:nos+2* and (F) the *nos-tub:nos+2(D)G:C* transgenes. Because nos^{BN} embryos lack endogenous *nos* mRNA (Wang et al., 1994), only the transgenic mRNA is detected.

protein in *Drosophila* S2 cells, the *Drosophila* protein has been previously referred to as Hrp59 (Kiesler et al., 2005). The phenotypes of a mutation we have generated in CG9373, described below, have led us to name this gene *rumpelstiltskin* (*rump*).

Recombinant Rump binds specifically to the +2′ element of the *nos* 3′UTR

The TRAP method is capable of purifying proteins that interact directly with the *nos* +2′ element RNA as well as proteins associated with the purified RNA-protein complex. To determine whether Rump interacts directly with the +2′ element, we tested the ability of purified full-length recombinant MBP-Rump fusion protein to bind to radiolabeled +2′ element RNA using a UV-crosslinking assay. MBP-Rump bound to the +2′ element, but not to the adjacent *nos* +1 localization element, indicating that the interaction with the +2′ element is specific (Fig. 2A). Crosslinking of MBP-Rump to the radiolabeled +2′ element RNA probe was competed by an excess of unlabeled +2′ RNA, but not by unlabeled +1 element RNA, verifying the specificity of MBP-Rump for +2′ element sequences (Fig. 2B).

To identify the binding site for Rump, several overlapping fragments of the +2′ element were assayed by UV-crosslinking to MBP-Rump (Fig. 2C). Binding of MBP-Rump to the 5′ half of the +2′ element (Δ2) was indistinguishable from binding to the full-length +2′ element, whereas no interaction was detected with the 3′ half (Δ5; Fig. 2C). Two non-overlapping subregions (Δ1 and Δ4) were each sufficient for binding by MBP-Rump, although binding was reduced relative to the overlapping Δ2 region or the full +2′ element (Fig. 2C). This result indicates the presence of multiple binding sites for Rump in the 5′ half of the +2′ element.

The Δ1 and Δ4 regions each contain a CGUU motif and linker-scanning mutations that overlap these motifs were previously shown to disrupt p75 binding and +2′ element function (Bergsten et al., 2001). To determine whether this sequence is recognized by Rump, a single G-to-C point mutation was introduced into each CGUU, individually or in combination [+2′(A)G:C, (D)G:C and (AD)G:C]. Either point mutation significantly disrupted binding of MBP-Rump to the +2′ element, when assayed by UV-crosslinking (Fig. 2C). By contrast, a linker-scanning mutation of six residues in the 3′ half of the +2′ element [+2′(F)] (Bergsten et al., 2001) had no detectable effect on MBP-Rump binding, consistent with the inability of the Δ5 fragment to bind to MBP-Rump (data not shown). Thus, binding of Rump to the wild-type +2′ element requires the integrity of both CGUU motifs. The context of these motifs is, however, important for Rump recognition, as little binding is detected using a synthetic RNA probe consisting solely of four CGUU repeats (data not shown).

To test whether Rump binding sites are required for localization, we introduced the (A)G:C and (D)G:C point mutations into the *nos-tub:nos+2* transgene (Fig. 2D). The *nos-tub:nos+2* transgene combines the +1 and +2′ elements, which act synergistically to confer substantial, albeit not wild-type, posterior localization (Gavis et al., 1996a). Because only two of the four *nos* localization elements are present in the *nos-tub:nos+2* transgene, localization signal redundancy is reduced. Thus, using this transgene permits us to assay the effects of +2′ element mutations on localization function. Both the (A)G:C and (D)G:C mutation, when tested individually or together, severely compromised posterior localization in 100% of embryos, consistent with their effect on Rump binding (Fig. 2E,F and data not shown). Together, these results suggest that Rump might function in vivo to regulate the posterior localization of *nos* mRNA through the +2′ element.

Isolation of a *rump* null allele

For analysis of Rump function in vivo, we raised monoclonal antibodies to recombinant Rump protein. In addition, we generated a *rump* mutation, $rump^{1}$, by excision of a *P* element inserted in the 5′UTR of CG9373 (Bellen et al., 2004). Imprecise excision of this *P* element produced a deletion beginning 426 nucleotides upstream and extending 501 nucleotides downstream of the insertion site (Fig. 3A). This lesion removes the transcription start site, the entire 5′UTR and the initial 152 codons, and is thus predicted to be a null mutation of CG9373. Homozygous $rump^{1}$ flies are viable through adulthood, facilitating analysis of *rump* mutant ovaries and embryos. In contrast to wild-type ovaries, ovaries from $rump^{1}$ mutant females lack detectable *rump* mRNA (Fig. 3B). Similarly, anti-Rump monoclonal antibodies fail to detect any Rump protein in mutant ovaries (Fig. 3C), indicating that $rump^{1}$ is a null mutation.

Homozygous $rump^{1}$ females showed a variable maternal-effect defect in the percentage of progeny that complete embryonic development, ranging from 29% (n=1137) to 65% (n=886). This

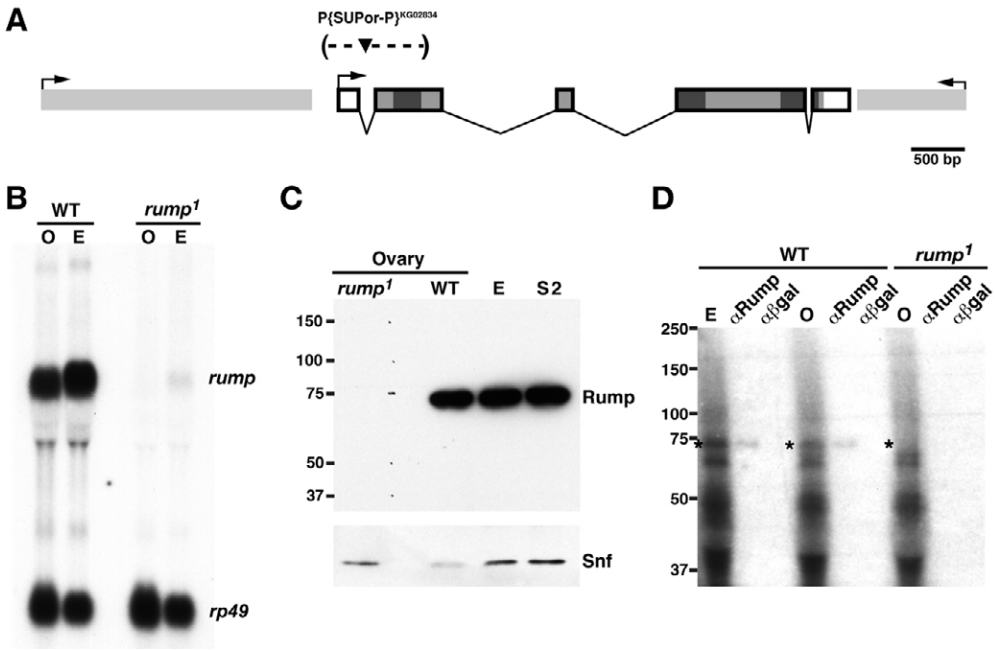

Fig. 3. Molecular characterization of *Drosophila rump* and generation of a *rump* null mutation. (**A**) Genomic region surrounding the CG9373/*rump* locus. The *rump* transcript is outlined by the thick black line, with the ORF (lighter shading) and three RRMs (darker shading) indicated. The arrowhead marks the *P* element insertion P{SUPor-P}^{KG02834} in the first intron and parentheses indicate the limits of the *rump*^{1} deletion (dashed line). Transcripts flanking the *rump* locus are shown in lightest gray. Arrows indicate direction of transcription. (**B**) Northern blot of total RNA from wild-type (WT) and *rump*^{1} ovaries (O) and 0- to 2-hour-old embryos (E), probed for *rump* and the loading control *rp49* (*RpL32* – FlyBase). The trace amount of *rump* detected in early embryos is due to contamination from zygotic *rump* expression. (**C**) Immunoblot of total protein from wild-type (WT) and *rump*^{1} ovaries, wild-type 0- to 2-hour embryos (E), and cultured Schneider cells (S2). Molecular mass standards are indicated in kDa. After transfer, the membrane was cut below the 37 kDa marker. The top portion was blotted with anti-Rump and the bottom with anti-Snf as a loading control. (**D**) UV-crosslinking of radiolabeled +2′ RNA to 0- to 2-hour embryo (E) or ovarian (O) extract from wild-type or *rump*^{1} animals. The position of the p75 binding activity (absent in *rump*^{1}) is marked with asterisks. UV-crosslinking reactions carried out in parallel were immunoprecipitated with anti-Rump (αRump) or a control anti-β-galactosidase (αβgal) antibody.

defect was rescued by a single copy of a genomic transgene containing only the *rump* transcription unit, with 80% (n=607) to 86% (n=1402) of the corresponding embryos hatching as larvae (P<0.001). Embryos displaying this and other maternal-effect defects will be referred to as *rump* mutant embryos. In addition to the maternal-effect defect, homozygous *rump* mutant males produced by parents heterozygous for *rump*^{1} exhibited reduced fertility. Further investigation of this phenotype showed that only 10% of males were able to fertilize virgin females within a 10-day period (n=29). Fertility was restored to 100% (n=30) by the *rump* transgene.

Rump corresponds to p75 binding activity and forms a complex with *nos* in vivo

The similarities in electrophoretic mobility of Rump and p75 and their recognition of the +2′ element CGUU motifs suggest that Rump corresponds to p75. To test whether the two are equivalent, we performed UV-crosslinking with a *nos* +2′ element probe and extract prepared from either wild-type embryos, wild-type ovaries or *rump*^{1} ovaries. As predicted, p75 binding activity was present in wild-type extract, but could not be detected in the *rump*^{1} extract (Fig. 3D). Furthermore, after UV-crosslinking, radiolabeled p75 could be immunoprecipitated with anti-Rump monoclonal antibody (Fig. 3D). These results show that Rump is the previously described p75 binding activity and confirm that the binding specificity exhibited by recombinant MBP-Rump mirrors that of the endogenous protein.

To determine whether Rump interacts with *nos* mRNA in vivo as well as in vitro, Rump was immunoprecipitated from wild-type or *rump* mutant ovary extract and RNA isolated from the immunoprecipitates was analyzed by RT-PCR using primers for *nos*. Polyadenylated *nos* mRNA was reproducibly detected in immunoprecipitates from wild-type ovary extract, but not in immunoprecipitates from *rump*^{1} ovary extract (Fig. 4A). In addition, a variety of control antibodies failed to immunoprecipitate *nos* mRNA (Fig. 4A and data not shown). To address whether the interaction between Rump and *nos* mRNA is maintained in the embryo, a similar co-immunoprecipitation experiment was performed using extract from 0- to 2-hour wild-type or *rump*^{1} embryos. RT-PCR showed that *nos* mRNA is also immunoprecipitated from embryonic extract by anti-Rump antibody in a Rump-dependent manner (Fig. 4B).

Rump protein is detected in ovaries and embryos

Immunoblotting experiments detected Rump in the ovary and early embryo (Fig. 3C), consistent with a role in *nos* mRNA localization. To determine the specific distribution of Rump, ovaries and embryos were stained with monoclonal anti-Rump antibodies. From the germarium onward, Rump was detected in the nuclei of the germline nurse cells and oocyte, as well as in the somatic follicle cell nuclei (Fig. 5A,B and data not shown). This distribution is consistent with the previously described nuclear localization of Rump in *Drosophila* S2 cells and of its ortholog Hrp59 in the *C. tentans* Balbiani ring system (Hase et al., 2006; Kiesler et al., 2005). We were unable to

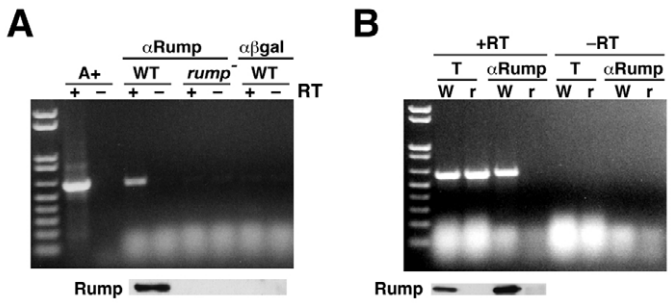

Fig. 4. Rump associates with *nos* mRNA in vivo. (**A**) RT-PCR to detect *nos* in RNA co-immunoprecipitated from wild-type (WT) and *rump*^{1} *Drosophila* ovaries with either anti-Rump or anti-β-galactosidase antibody. Poly(A+) RNA serves as positive control for RT-PCR. Reactions were performed with (+) and without (–) reverse transcriptase and products were visualized with ethidium bromide. Molecular weight standards in the first lane correspond to the 1 kb-Plus Ladder (Invitrogen). Beneath is shown an immunoblot of protein from each IP sample with anti-Rump antibody. (**B**) RT-PCR for *nos* (top) and anti-Rump immunoblot (bottom) as in A. Samples from WT (W) and *rump*^{1} (r) 0- to 2-hour embryos are indicated. Reactions were carried out with (+) or without (–) reverse transcriptase (RT) using total RNA (T) from the extracts used for IP as a positive control or RNA co-immunoprecipitated with anti-Rump antibody.

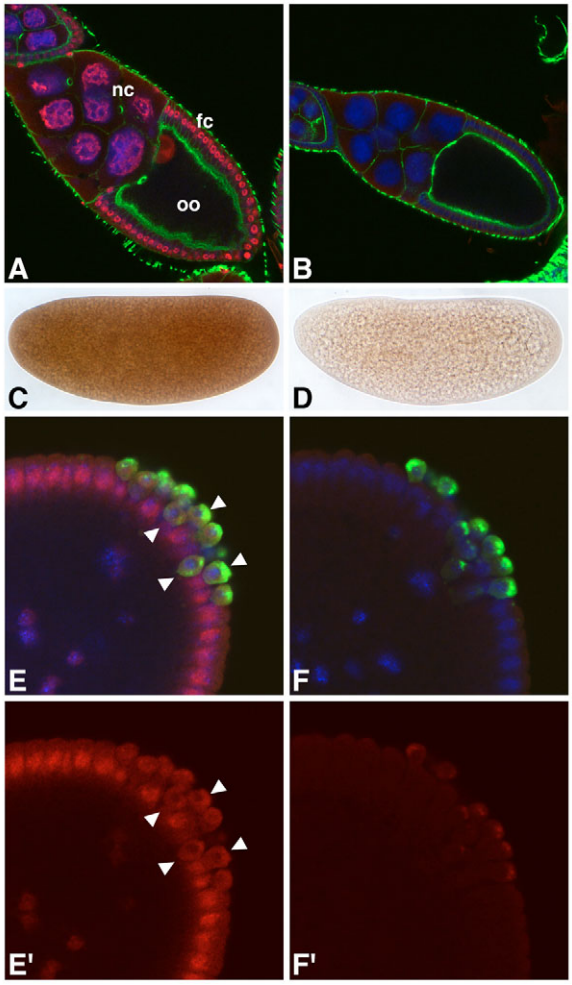

Fig. 5. Distribution of Rump protein in *Drosophila* ovaries and embryos. (**A**,**B**) Confocal images of stage-10 egg chambers from wild-type (A) and *rump*^{1} (B) females stained with anti-Rump antibody (red). The actin cytoskeleton is visualized in green, DNA in blue. nc, nurse cells; fc, follicle cells; oo, oocyte. (**C**,**D**) Immunohistochemical staining of preblastoderm wild-type (C) and *rump*^{1} (D) embryos with anti-Rump antibody. (**E-F′**) Confocal images showing the posterior poles of blastoderm-stage wild-type (E) and *rump*^{1} (F) embryos stained with anti-Rump (red) and anti-Vas (green). DNA is in blue. (E′,F′) Red channel (Rump) only from E and F. In wild-type embryos, Rump is detected cytoplasmically and in all somatic nuclei, but it is specifically absent from nuclei of pole cells, which are marked by Vas (arrowheads).

detect cytoplasmic staining above background levels in the ovary. In the newly fertilized embryo, Rump was present throughout the cytoplasm (Fig. 5C,D). Just prior to cellularization, Rump could be detected in both the somatic blastoderm nuclei and their surrounding cytoplasm, as well as in the internal yolk nuclei (Fig. 5E,F). However, it was noticeably excluded from the nuclei of the germline precursors, the pole cells, which are marked by Vas (Fig. 5E′,F′). This nuclear exclusion was maintained during the subsequent migration of the pole cells to the interior of the embryo (data not shown).

rump mutant embryos display abdominal patterning defects

The interaction of Rump with *nos* mRNA in vivo and the ability of Rump to recognize the *nos* +2′ element in vitro support a role for Rump as a *nos* mRNA localization factor. *rump*^{1} homozygous embryos exhibited a weak, though significant, segmentation defect that was rescued by the *rump* transgene, although this phenotype was variable in its penetrance (Fig. 6A). Such a mild defect is unsurprising given the redundancy of localization elements in the *nos* 3′UTR, as elimination of factors that recognize individual elements would be expected to produce only minor effects on *nos* localization. To devise a more sensitive assay for defects in *nos* localization, we reasoned that reducing the levels of *nos* mRNA would sensitize the embryo to defects in the *nos* localization machinery. Indeed, reducing *nos* gene dosage to one copy in *rump* mutant embryos significantly increased both the frequency and severity of abdominal segmentation defects (Fig. 6A). The fourth and fifth abdominal segments, which are most sensitive to a reduction of *nos* activity, were most frequently affected in this assay, consistent with a defect in *nos* localization. Importantly, loss of *rump* did not affect posterior localization of *osk* mRNA, Osk protein level, or posterior accumulation of Vas (see Fig. S1 in the supplementary material), supporting a direct effect on *nos*.

To complement the above analysis, we partially compromised the *nos* localization machinery by using a null mutation in the germ plasm component *tudor* (*tud*^{tux46}) (Thomson and Lasko, 2004). In embryos heterozygous for *tud*^{tux46}, *nos* levels were unchanged, but mild abdominal patterning defects were observed in a small percentage (4%) of embryos (Fig. 6B and data not shown). Elimination of one or both copies of *rump* in this sensitized genetic background resulted in an enhancement of the abdominal segmentation defects in a dosage-dependant manner, with 44% of embryos showing segmental deletions and fusions in the absence of *rump* (Fig. 6B and data not shown). Similar results were observed using a second *tud* allele (*tud*^{WC8}, data not shown). Once again, the fourth and fifth abdominal segments were most often affected, consistent with a role for *rump* in the regulation of posterior *nos* activity.

Finally, we reduced *nos* localization signal redundancy by using the *nos-tub:nos+2* transgene (Gavis et al., 1996a; described above), which confers substantial, albeit not wild-type, posterior localization. Since this transgene includes sequences required for

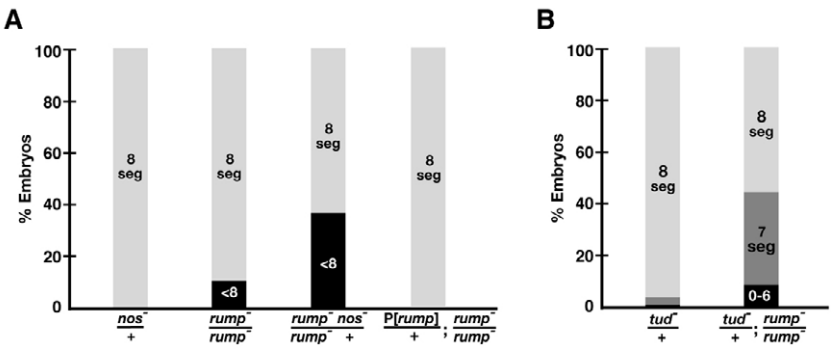

Fig. 6. Phenotypic analysis of *rump*. Bar charts show distributions of embryonic cuticle phenotypes for the population of *Drosophila* embryos that complete embryonic development, binned by the number of abdominal segments produced. For each graph, embryos from different genotypes were collected in parallel under the same conditions and over the same time period. The statistical significance of differences observed between pairs of genotypes was determined using the χ^2 test. (**A**) Embryos with eight complete segments (8 seg) were binned separately from those containing partial or entire segment deletions (<8, black) for each genotype. nos^{BN} heterozygotes (nos^-/+) do not display segmentation defects (n=210). The $rump^1$ distribution (n=332) differs significantly from nos^-/+ or wild-type (not shown) (P<0.001). A single copy of a genomic *rump* transgene, *P[rump]*, rescues the *rump* defect (n=483, P<0.001 versus $rump^1$). Removing a single copy of *nos* from $rump^1$ embryos using a $rump^1$ nos^{BN} recombinant chromosome in trans to $rump^1$ ($rump^-$ nos^-/$rump^-$ +, n=867) increases the percentage of defective embryos beyond that of *rump* mutants alone (37% versus 11%, P<0.001). Similar results were obtained using the $rump^1$ nos^{BN} recombinant chromosome in combination with either of three deficiencies that delete *rump* (data not shown). (**B**) Embryos were binned with: eight complete segments (8 seg); seven complete segments or seven to eight segments with partial deletions (7 seg); six or fewer segments (0-6). tud^{tux46} heterozygotes (tud^-/+) exhibit a low percentage of abdominal defects (n=367). When *rump* is eliminated (tud^-/+; $rump^-$/$rump^-$, n=266), the frequency and severity of abdominal defects are significantly increased (P<0.001).

nos translational control, all of the *nos* activity that is produced results from the translation of localized *nos-tub:nos+2* mRNA (Gavis et al., 1996b). A single copy of the *nos-tub:nos+2* transgene partially rescued the abdominal defects of *nos* mutant embryos, such that the majority developed four or more abdominal segments and over 30% were nearly wild-type, with seven to eight segments (Fig. 7A). In the absence of *rump*, the ability of the *nos-tub:nos+2* transgene to rescue abdominal segmentation was severely compromised and more than 90% of embryos developed fewer than four abdominal segments (Fig. 7A). As a molecular measure of abdominal segmentation, we monitored expression of the pair-rule gene *even-skipped* (*eve*), which is expressed in seven stripes corresponding to even-numbered segments (Macdonald et al., 1986). *nos* mutant embryos expressing *nos-tub:nos+2* had four to seven *eve* stripes, with over 60% of embryos displaying the complete set of seven stripes (Fig. 7B). In the absence of *rump*, this distribution was shifted, such that the majority of embryos (66%) had fewer than seven stripes (Fig. 7B). Eve stripes four to seven, which designate the abdomen, were most sensitive to loss of *rump* (Fig. 7C), consistent with the abdominal segmentation defects of these larvae.

rump mutants reduce *nos* mRNA localization to the embryo posterior

We hypothesized that the reduction in posterior *nos* activity in *nos-tub:nos+2* embryos lacking *rump* results from decreased posterior localization of *nos-tub:nos+2* mRNA. We therefore carried out in situ hybridization to *nos-tub:nos+2* mRNA in the presence or absence of *rump*. Consistent with the partial rescue exhibited by the *nos-tub:nos+2* transgene, *nos-tub:nos+2* mRNA showed variable posterior localization, although the majority of embryos (77%) had qualitatively 'substantial' (++) localization and only 1% of embryos showed no detectable (–) posterior localization (Fig. 7D,E). However, in the absence of *rump*, only 42% of embryos showed 'substantial' posterior localization of *nos-tub:nos+2* RNA, whereas 38% showed weak (+) or diffuse localization and 20% of embryos had no detectable localization (Fig. 7D,E). Thus, the abdominal segmentation defects observed with loss of *rump* can be explained by loss of *nos* mRNA localization. Moreover, these results demonstrate a role for *rump* in *nos* mRNA localization.

DISCUSSION

Using a biochemical approach, we have identified Rump, the *Drosophila* hnRNP M homolog, as a bona fide *nos* mRNA localization factor. Rump corresponds to the p75 binding activity that was previously shown to recognize the *nos* +2′ localization element (Bergsten et al., 2001). Recombinant and endogenous Rump recognize two CGUU motifs in the +2′ element. A point mutation within either of these motifs is sufficient to disrupt both interaction with Rump and mRNA localization function. The demonstration that sequences required for Rump binding are also required for posterior localization provides strong evidence that Rump plays a direct role in mediating *nos* mRNA localization through its interaction with the *nos* 3′UTR.

Rump was previously identified in *Drosophila* S2 cells through its cross-reactivity with an antibody to the orthologous *C. tetans* protein, Hrp59 (Kiesler et al., 2005). In our experiments, *Drosophila* ovarian, embryonic and S2-cell Rump protein migrate with an apparent mobility of ~70 kDa, consistent with its calculated molecular weight of 67 kDa. Mammalian hnRNP M proteins have been implicated in splicing through their association with pre-mRNA at an early step in spliceosome assembly (Kafasla et al., 2002). Studies in *Chironomus* have shown that Hrp59 binds to pre-mRNA co-transcriptionally and remains associated with the RNA until it reaches the nuclear envelope, and recent analysis of the *Drosophila* S2 cell protein shows that it regulates alternative splicing of its own mRNA (Hase et al., 2006; Kiesler et al., 2005).

Our results indicate that Rump has multiple functions at various stages of the *Drosophila* life cycle. In addition to defects in abdominal segmentation, many embryos produced by *rump* mutant females arrest development prematurely and adult *rump* mutant males are largely sterile. Neither the maternal-effect developmental arrest nor the zygotic sterility phenotypes is characteristic of *nos* mutants, indicating that Rump regulates both *nos*-dependent and *nos*-independent processes. This functional pleiotropy is consistent with the isolation of numerous Rump target mRNAs from S2 cells, the steady state levels of which are decreased by RNAi knockdown of *rump* (Kiesler et al., 2005). Since *nos* is not expressed in S2 cells, its behavior in this assay cannot be determined. However, we detect no alteration in the abundance or splicing of *nos* mRNA in *rump*

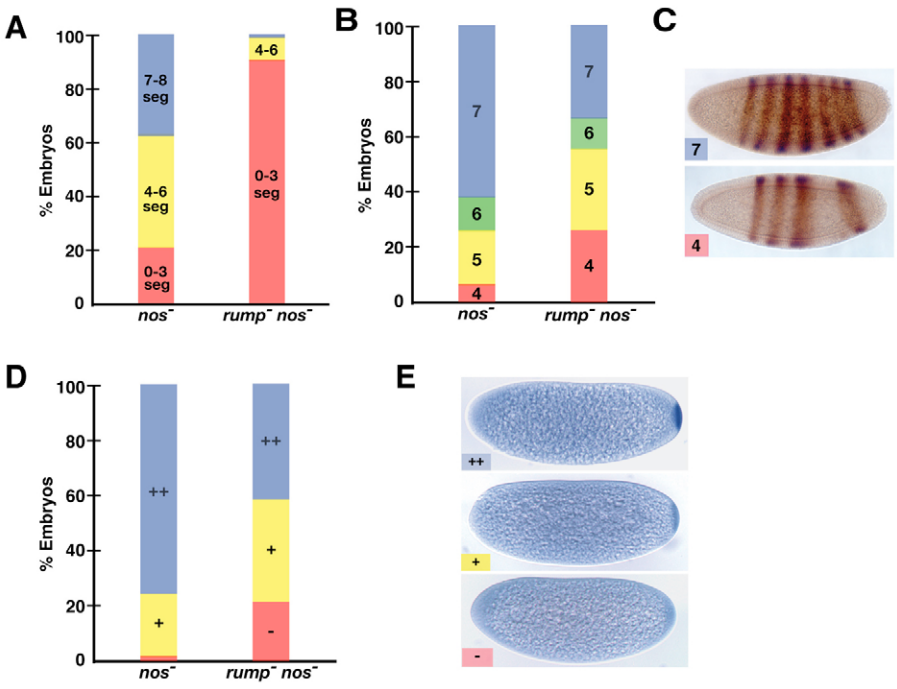

Fig. 7. Rump regulates posterior localization of *nos* mRNA. The *nos-tub:nos+2* transgene (see Fig. 2D) was introduced into either nos^{BN} or $rump^{1}$ nos^{BN}/*Df(rump)* nos^{BN} *Drosophila* females and provides the sole source of maternal *nos* mRNA. (**A**) Embryos that develop to produce cuticle were binned as follows: seven or eight partial or complete segments (7-8 seg); four, five or six partial or complete segments (4-6 seg); three or fewer segments (0-3 seg). The *nos-tub:nos+2* transgene produces embryos with a range of segmentation (nos^{-}, *n*=455). When *rump* is eliminated, segmentation is significantly reduced (nos^{-} $rump^{-}$, *n*=220, *P*<0.001). (**B**,**C**) Eve-stained embryos were binned according to the number of Eve stripes observed in the presence (*n*=153) or absence (*n*=212) of *rump* (*P*<0.001). Embryos representative of seven- and four-stripe bins are shown in C. (**D**,**E**) Posterior localization of *nos-tub:nos+2* RNA was evaluated by in situ hybridization to 0- to 2-hour embryos and classified as substantial (++), weak or diffuse (+), or undetectable (–) as illustrated in E. Localization is significantly reduced by elimination of *rump* (nos^{-}, *n*=382; nos^{-} $rump^{-}$, *n*=417, *P*<0.001).

mutant ovaries or embryos. Instead, our data demonstrate a specific and previously unidentified role for Rump as an mRNA localization factor.

The different regulatory functions of Rump might be distinguished by distinct recognition motifs in Rump target mRNAs. Rump protein isolated from S2 cells by immunoprecipitation with anti-Hrp59 antibody binds preferentially to a purine-rich motif with similarity to exonic splicing enhancers. This motif, with GGAGG at its core, is enriched among Rump target mRNAs in S2 cells identified by whole-genome analysis (Kiesler et al., 2005). The GGAGG core sequence does not exist within the *nos* +2′ element, nor within the entire *nos* 3′UTR. The ability to recognize different motifs might be conferred by different RRMs within Rump. Similarity between RRM3 and the human splicing regulator ASF (also known as SF2 and SFRS1 – Human Gene Nomenclature Database) RRM suggests that RRM3 might be specifically responsible for interaction with splicing targets (Kiesler et al., 2005), whereas RRMs 1 and/or 2 might recognize a different set of Rump targets. In addition, binding of Rump to *nos* might be cooperative, as mutation of one or both CGUU motifs is equally deleterious. Consistent with this idea, Rump self-interaction was detected in a yeast two-hybrid screen (Giot et al., 2003), suggesting that Rump might function as a dimer.

Multifunctionality appears to be a common feature of proteins that regulate mRNA localization and localized translation. For example, *Drosophila* Hrp48 (also known as Hrb27C – FlyBase), an hnRNP A/B family member that participates in localization and translational regulation of *osk* and *gurken* mRNAs (Goodrich et al., 2004; Huynh et al., 2004; Norvell et al., 2005; Norvell et al., 1999; Yano et al., 2004), also functions as a regulator of alternative splicing (Hammond et al., 1997) and mammalian homologs of *Xenopus* Vg1RBP60, an hnRNP I protein involved in *Vg1* mRNA localization (Cote et al., 1999), play various roles in nuclear RNA biogenesis (Valcarcel and Gebauer, 1997). Similarly to Rump, activities of two other *nos* regulators, Glorund (Glo) and Smaug (Smg), may be distinguished through multiple, distinct binding specificities. Glo, an hnRNP F/H homolog, represses translation of unlocalized *nos* during oogenesis through its interaction with an AU-rich double-stranded region within the *nos* 3′UTR (Kalifa et al., 2006), whereas its mammalian counterparts regulate alternative splicing through their interaction with a G-rich motif (Caputi and Zahler, 2001; Matunis et al., 1994). Smg represses translation of unlocalized *nos* in the embryo through its interaction with Smaug Recognition Elements (SREs) in the *nos* 3′UTR (Crucs et al., 2000; Dahanukar et al., 1999; Smibert et al., 1999), but its function in degradation of maternal mRNAs is SRE-independent (Semotok et al., 2005).

Elimination of *rump* function has a more variable effect on localization of *nos-tub:nos+2* RNA than does mutation of Rump binding sites. Thus, another ovarian protein with a similar recognition motif might be able to compensate for the loss of Rump. Alternatively, mutation of the Rump binding site(s) might have a more global effect on the structure of the localization element, disrupting the function of other localization factors. The CGUU motifs recognized by Rump flank one of the two SREs recognized by Smg within the *nos* 3′UTR and both the (A)G:C and (D)G:C mutations disrupt the function of the SRE, consistent with the ability of these mutations to cause pleiotropic effects. By contrast, mutation of the SRE had only a small effect on p75 binding to the +2′ element (Bergsten et al., 2001), suggesting that Rump binding is less sensitive to local perturbations. Finally, several linker-scanning mutations in the +2′ element disrupt the localization function of this element but do not disrupt Rump binding in vitro (Bergsten et al., 2001) (our results), suggesting that at least one additional, as yet unknown, factor mediates localization via the +2′ element.

During early and mid-oogenesis, Rump accumulates in the nurse cell nuclei where *nos* is synthesized, suggesting that it might first associate with *nos* mRNA in the nucleus. In this regard, Rump may

resemble *Xenopus* Vg1RBP60/hnRNP I, which associates with *Vg1* and *VegT* mRNAs in the nucleus and travels with the RNAs to the cytoplasm where the RNP is remodeled (Kress et al., 2004). Owing to the impenetrability of the late-stage oocyte to antibodies, we have not been able to determine the distribution of Rump in late oocytes when *nos* becomes posteriorly localized. However, Rump appears cytoplasmic in newly fertilized embryos and is not enriched at the posterior of the embryo, suggesting that it does not maintain a stable association with *nos* once anchored at the germ plasm. Biochemical evidence for a continued association of Rump with *nos* during embryogenesis, together with the uniform distribution of Rump protein, indicate that in the early embryo Rump is most likely to be associated with unlocalized, translationally repressed *nos* mRNA. The close apposition of Rump and Smg binding sites raises the possibility that binding by these factors is mutually stabilizing.

Taken together, data presented here suggest a model whereby Rump associates with *nos* mRNA during oogenesis, possibly in the nucleus, where it participates in the generation or stabilization of localization-competent *nos* RNP complexes. A small fraction of *nos* RNPs are entrapped by the germ plasm and this association results in reorganization of the RNP and release of Rump. The majority of *nos* mRNA remains unlocalized and, consequently, bound to Rump. Whether Rump plays a role in coordinating translational control with *nos* mRNA localization remains to be determined.

We thank S. Chatterjee for help with protein purification, fly work and, with M. Klosinska, for help with monoclonal antibody screening; S. Kyin (Princeton Mass Spectrometry Facility); C. DeCoste and J. Levorse (Princeton Monoclonal Facility); J. Goodhouse (Princeton Microscopy Facility); C. Schwartz and H. Krause for the TRAP vector and advice on purification; T. Thomson and P. Lasko for the *tud*^{tux46} allele; P. Schedl, R. Lehmann and A. Ephrussi for antibodies; and T. Weil and K. Sinsimer for comments on the manuscript. This work was supported by an NSF Predoctoral Fellowship (R.A.J.) and a grant from the National Institutes of Health (GM067758).

Supplementary material

Supplementary material for this article is available at http://dev.biologists.org/cgi/content/full/135/5/973/DC1

References

Bellen, H. J., Levis, R. W., Liao, G., He, Y., Carlson, J. W., Tsang, G., Evans-Holm, M., Hiesinger, P. R., Schulze, K. L., Rubin, G. M. et al. (2004). The BDGP gene disruption project: single transposon insertions associated with 40% of *Drosophila* genes. *Genetics* **167**, 761-781.

Bergsten, S. E. and Gavis, E. R. (1999). Role for mRNA localization in translational activation but not spatial restriction of *nanos* RNA. *Development* **126**, 659-669.

Bergsten, S. E., Huang, T., Chatterjee, S. and Gavis, E. R. (2001). Recognition and long-range interactions of a minimal *nanos* RNA localization signal element. *Development* **128**, 427-435.

Berleth, T., Burri, M., Thoma, G., Bopp, D., Richstein, S., Frigerio, G., Noll, M. and Nüsslein-Volhard, C. (1988). The role of localization of *bicoid* RNA in organizing the anterior pattern of the *Drosophila* embryo. *EMBO J.* **7**, 1749-1756.

Caputi, M. and Zahler, A. M. (2001). Determination of the RNA binding specificity of the heterogeneous nuclear ribonucleoprotein (hnRNP) H/H'/F/2H9 family. *J. Biol. Chem.* **276**, 43850-43859.

Cha, B. J., Koppetsch, B. S. and Theurkauf, W. E. (2001). In vivo analysis of *Drosophila bicoid* mRNA localization reveals a novel microtubule-dependent axis specification pathway. *Cell* **106**, 35-46.

Chan, A. P., Kloc, M. and Etkin, L. D. (1999). fatvg encodes a new localized RNA that uses a 25-nucleotide element (FVLE1) to localize to the vegetal cortex of *Xenopus* oocytes. *Development* **126**, 4943-4953.

Cote, C. A., Gautreau, D., Denegre, J. M., Kress, T., Terry, N. A. and Mowry, K. L. (1999). A *Xenopus* protein related to hnRNP I has a role in cytoplasmic RNA localization. *Mol. Cell* **4**, 431-437.

Crucs, S., Chatterjee, S. and Gavis, E. R. (2000). Overlapping but distinct RNA elements control repression and activation of *nanos* translation. *Mol. Cell* **5**, 457-467.

Dahanukar, A., Walker, J. A. and Wharton, R. P. (1999). Smaug, a novel RNA-binding protein that operates a translational switch in *Drosophila*. *Mol. Cell* **4**, 209-218.

Driever, W. and Nüsslein-Volhard, C. (1988). A gradient of bicoid protein in *Drosophila* embryos. *Cell* **54**, 83-93.

Driever, W. and Nüsslein-Volhard, C. (1989). The bicoid protein is a positive regulator of hunchback transcription in the early *Drosophila* embryo. *Nature* **337**, 138-143.

Dubnau, J. and Struhl, G. (1996). RNA recognition and translational regulation by a homeodomain protein. *Nature* **379**, 694-699.

Duchow, H. K., Brechbiel, J. L., Chatterjee, S. and Gavis, E. R. (2005). The *nanos* translational control element represses translation in somatic cells by a Bearded box-like motif. *Dev. Biol.* **282**, 207-217.

Forbes, A. and Lehmann, R. (1998). Nanos and Pumilio have critical roles in the development and function of *Drosophila* germline stem cells. *Development* **125**, 679-690.

Forrest, K. M. and Gavis, E. R. (2003). Live imaging of endogenous mRNA reveals a diffusion and entrapment mechanism for *nanos* mRNA localization in *Drosophila*. *Curr. Biol.* **13**, 1159-1168.

Gattoni, R., Mahe, D., Mahl, P., Fischer, N., Mattei, M. G., Stevenin, J. and Fuchs, J. P. (1996). The human hnRNP-M proteins: structure and relation with early heat shock-induced splicing arrest and chromosome mapping. *Nucleic Acids Res.* **24**, 2535-2342.

Gautreau, D., Cote, C. A. and Mowry, K. L. (1997). Two copies of a sub-element from the Vg1 RNA localization sequence are sufficient to direct vegetal localization in *Xenopus* oocytes. *Development* **124**, 5013-5020.

Gavis, E. R. and Lehmann, R. (1992). Localization of *nanos* RNA controls embryonic polarity. *Cell* **71**, 301-313.

Gavis, E. R. and Lehmann, R. (1994). Translational regulation of *nanos* by RNA localization. *Nature* **369**, 315-318.

Gavis, E. R., Curtis, D. and Lehmann, R. (1996a). Identification of cis-acting sequences that control *nanos* RNA localization. *Dev. Biol.* **176**, 36-50.

Gavis, E. R., Lunsford, L., Bergsten, S. E. and Lehmann, R. (1996b). A conserved 90 nucleotide element mediates translational repression of *nanos* RNA. *Development* **122**, 2791-2800.

Gavis, E. R., Singer, R. H. and Hüttelmaier, S. (2007). Localized translation through messenger RNA localization. In *Translational Control* (ed. J. W. B. Hershey, M. B. Mathews and N. Sonenberg), pp. 687-717. Cold Spring Harbor, NY: Cold Spring Harbor Laboratory Press.

Gavis, E. R., Chatterjee, S., Ford, N. R. and Wolff, L. J. (2008). Dispensability of *nanos* mRNA localization for abdominal patterning but not for germ cell development. *Mech. Dev.* **125**, 81-90.

Giot, L., Bader, J. S., Brouwer, C., Chaudhuri, A., Kuang, B., Li, Y., Hao, Y. L., Ooi, C. E., Godwin, B., Vitols, E. et al. (2003). A protein interaction map of *Drosophila melanogaster*. *Science* **302**, 1727-1736.

Gonzalez, I., Buonomo, S. B., Nasmyth, K. and von Ahsen, U. (1999). *ASH1* mRNA localization in yeast involves multiple secondary structural elements and Ash1 protein translation. *Curr. Biol.* **9**, 337-340.

Goodrich, J. S., Clouse, K. N. and Schüpbach, T. (2004). Hrb27C, Sqd and Otu cooperatively regulate *gurken* RNA localization and mediate nurse cell chromosome dispersion in *Drosophila* oogenesis. *Development* **131**, 1949-1958.

Hammond, L. E., Rudner, D. Z., Kanaar, R. and Rio, D. C. (1997). Mutations in the *hrp48* gene, which encodes a *Drosophila* heterogeneous nuclear ribonucleoprotein particle protein, cause lethality and developmental defects and affect P-element third-intron splicing in vivo. *Mol. Cell. Biol.* **17**, 7260-7267.

Hase, M. E., Yalamanchili, P. and Visa, N. (2006). The *Drosophila* heterogeneous nuclear ribonucleoprotein M protein, HRP59, regulates alternative splicing and controls the production of its own mRNA. *J. Biol. Chem.* **281**, 39135-39141.

Hülskamp, M. and Tautz, D. (1991). Gap genes and gradients-the logic behind the gaps. *BioEssays* **13**, 261-268.

Huynh, J. R., Munro, T. P., Smith-Litiere, K., Lepesant, J. A. and St Johnston, D. S. (2004). The *Drosophila* hnRNPA/B homolog, Hrp48, is specifically required for a distinct step in *osk* mRNA localization. *Dev. Cell* **6**, 625-635.

Kafasla, P., Patrinou-Georgoula, M., Lewis, J. D. and Guialis, A. (2002). Association of the 72/74-kDa proteins, members of the heterogeneous nuclear ribonucleoprotein M group, with the pre-mRNA at early stages of spliceosome assembly. *Biochem. J.* **363**, 793-799.

Kalifa, Y., Huang, T., Rosen, L. N., Chatterjee, S. and Gavis, E. R. (2006). Glorund, an hnRNP F/H homolog, is an ovarian repressor of *nanos* translation. *Dev. Cell* **10**, 291-301.

Kiesler, E., Hase, M. E., Brodin, D. and Visa, N. (2005). Hrp59, an hnRNP M protein in *Chironomus* and *Drosophila*, binds to exonic splicing enhancers and is required for expression of a subset of mRNAs. *J. Cell Biol.* **168**, 1013-1025.

Kobayashi, S., Yamada, M., Asaoka, M. and Kitamura, T. (1996). Essential role of the posterior morphogen *nanos* for germline development in *Drosophila*. *Nature* **380**, 708-711.

Kress, T. L., Yoon, Y. J. and Mowry, K. L. (2004). Nuclear RNP complex assembly initiates cytoplasmic RNA localization. *J. Cell Biol.* **165**, 203-211.

Macdonald, P. M. and Kerr, K. (1998). Mutational analysis of an RNA recognition element that mediates localization of *bicoid* mRNA. *Mol. Cell. Biol.* **18**, 3788-3795.

Macdonald, P. M., Ingham, P. and Struhl, G. (1986). Isolation, structure, and expression of *even-skipped*: a second pair-rule gene of *Drosophila* containing a homeo box. *Cell* **47**, 721-734.
Mansfield, J. H., Wilhelm, J. E. and Hazelrigg, T. (2002). Ypsilon Schachtel, a *Drosophila* Y-box protein, acts antagonistically to Orb in the *oskar* mRNA localization and translation pathway. *Development* **129**, 197-209.
Matunis, M. J., Xing, J. and Dreyfuss, G. (1994). The hnRNP F protein: unique primary structure, nucleic acid-binding properties, and subcellular localization. *Nucleic Acids Res.* **22**, 1059-1067.
Nelson, M. R., Luo, H., Vari, H. K., Cox, B. J., Simmonds, A. J., Krause, H. M., Lipshitz, H. D. and Smibert, C. A. (2007). A multiprotein complex that mediates translational enhancement in *Drosophila*. *J. Biol. Chem.* **282**, 34031-34038.
Norvell, A., Kelley, R. L., Wehr, K. and Schüpbach, T. (1999). Specific isoforms of *squid*, a *Drosophila* hnRNP, perform distinct roles in Gurken localization during oogenesis. *Genes Dev.* **13**, 864-876.
Norvell, A., Debec, A., Finch, D., Gibson, L. and Thoma, B. (2005). Squid is required for efficient posterior localization of *oskar* mRNA during *Drosophila* oogenesis. *Dev. Genes Evol.* **215**, 340-349.
Rivera-Pomar, R., Niessing, D., Schmidt-Ott, U., Gehring, W. J. and Jäckle, H. (1996). RNA binding and translational suppression by bicoid. *Nature* **379**, 746-749.
Semotok, J. L., Cooperstock, R. L., Pinder, B. D., Vari, H. K., Lipshitz, H. D. and Smibert, C. A. (2005). Smaug recruits the CCR4/POP2/NOT deadenylase complex to trigger maternal transcript localization in the early *Drosophila* embryo. *Curr. Biol.* **15**, 284-294.
Shcherbata, H. R., Althauser, C., Findley, S. D. and Ruohola-Baker, H. (2004). The mitotic-to-endocycle switch in *Drosophila* follicle cells is executed by Notch-dependent regulation of G1/S, G2/M and M/G1 cell-cycle transitions. *Development* **131**, 3169-3181.
Smibert, C. A., Lie, Y. S., Shillingaw, W., Henzel, W. J. and Macdonald, P. M. (1999). Smaug, a novel and conserved protein contributes to repression of *nanos* mRNA translation in vitro. *RNA* **5**, 1535-1547.
Song, Y., Fee, L., Lee, T. H. and Wharton, R. P. (2007). The molecular chaperone Hsp90 is required for mRNA localization in *Drosophila melanogaster* embryos. *Genetics* **176**, 2213-2222.
Spradling, A. C. (1986). P element-mediated transformation. In *Drosophila: A Practical Approach* (ed. D. B. Roberts), pp. 175-197. Oxford: IRL Press.
St Johnston, D. (2005). Moving messages: the intracellular localization of mRNAs. *Nat. Rev. Mol. Cell Biol.* **6**, 363-375.
Struhl, G., Struhl, K. and Macdonald, P. M. (1989). The gradient morphogen *bicoid* is a concentration-dependent transcriptional activator. *Cell* **57**, 1259-1273.
Tautz, D. and Pfeifle, C. (1989). A non-radioactive in situ hybridization method for the localization of specific RNAs in *Drosophila* embryos reveals translational control of the segmentation gene *hunchback*. *Chromosoma* **98**, 81-85.
Thomson, T. and Lasko, P. (2004). *Drosophila tudor* is essential for polar granule assembly and pole cell specification, but not for posterior patterning. *Genesis* **40**, 164-170.
Valcarcel, J. and Gebauer, F. (1997). Post-transcriptional regulation: the dawn of PTB. *Curr. Biol.* **7**, R705-R708.
Wang, C. and Lehmann, R. (1991). *Nanos* is the localized posterior determinant in *Drosophila*. *Cell* **66**, 637-647.
Wang, C., Dickinson, L. K. and Lehmann, R. (1994). Genetics of *nanos* localization in *Drosophila*. *Dev. Dyn.* **199**, 103-115.
Wang, Z. and Lin, H. (2004). Nanos maintains germline stem cell self-renewal by preventing differentiation. *Science* **303**, 2016-2019.
Weil, T. T., Forrest, K. M. and Gavis, E. R. (2006). Localization of *bicoid* mRNA in late oocytes is maintained by continual active transport. *Dev. Cell* **11**, 251-262.
Wharton, R. P. and Struhl, G. (1989). Structure of the *Drosophila* BicaudalD protein and its role in localizing the posterior determinant *nanos*. *Cell* **59**, 881-892.
Yano, T., de Quinto, S. L., Matsui, Y., Shevchenko, A. and Ephrussi, A. (2004). Hrp48, a *Drosophila* hnRNPA/B homolog, binds and regulates translation of *oskar* mRNA. *Dev. Cell.* **6**, 637-648.
Ye, B., Petritsch, C., Clark, I. E., Gavis, E. R., Jan, L. Y. and Jan, Y. N. (2004). *nanos* and *pumilio* are essential for dendrite morphogenesis in *Drosophila* peripheral neurons. *Curr. Biol.* **14**, 314-321.